BAUET JOURNAL
Published by
Bangladesh Army University of Engineering & Technology
Journal Homepage: http://journal.bauet.ac.bd

Environmental Risk Zone Identification of An Urban Unit Using GIS And Remote Sensing

Md. Nazmul Haque[1, *], Syed Riad Morshed[1], Md. Abdul Fattah[1], Afiya Kashem Ishra[1], Md. Mustafa Saroar[1]

[1]Department of Urban and Regional Planning, Faculty of Civil Engineering, Khulna University of Engineering and Technology, 9203, Khulna, Bangladesh

Abstract: Massive changes in landforms due to the rapid pace of urbanization over the last couple of decades have caused extensive damage to the urban environment in most large cities in Bangladesh; Khulna city is of no exception. This study aimed to identify the areas at most risk, taking the north-west part of Khulna city as a study unit. Accordingly, an environmental risk assessment largely focused on the temporal changes in physical and meteorological aspects that were done for the period 2003 to 2019. To develop the physical profiles of the study unit, this study has used elevation data available on Google Earth. ArcGIS is used to visualize the changes in topography, slope, and other variables for the study period. The changes in meteorological variables such as rainfall, temperature and relative humidity have been analyzed in a GIS environment. GIS-based Landsat image classification shows that the build-up area has increased 11% in the study unit. The land surface temperature (LST) model shows that temperature has increased in 55.3% areas and the average increase is 2°C during the study period. The areas at most risk have been identified and visualized using the Weighted Overlay function in ArcGIS. The findings of the study would help the city planning and management authorities to initiate an informed intervention for making Khulna city safe, resilient, and sustainable in line with sustainable development goal 11 (SDG 11).

Keywords: *Environmental assessment; Land use; Meteorological change; Weighted Overlay.*

Introduction: Environmental concern has become one of the major global alarms that individually and/or collectively impact all nations [1]. With the increase of population and unplanned urban expansion, land use patterns and ecosystems have changed, leading to a series of urban-oriented environmental challenges around the world [2,12]. Land use and land cover (LULC) type have been changing rapidly due to many driving forces [22]. As a result, carbon emissions, climate change, alternation of ecosystems, environmental degradation, and the haphazard condition has been increasing which makes the environment of any area unsuitable for human habitation [3, 4].

Bangladesh is one of the world's highly populated countries, where urban populations have grown over time as a result of migration for employment opportunities and better quality of life [5,14]. As a result, the percentage of the buildup area such as residential, commercial, industrial, and other types of infrastructures, has increased manifold in the last few decades in the major cities of the country such as Dhaka, Chittagong, Khulna, and Rajshahi. Literature shows that most of these cities including Khulna city have been facing deteriorated environmental quality and livability resulted from traffic congestion, noise, air, and water pollution, waterlogging [6,11], increased surface temperature [7, 8, 9] and degradation of ecosystem component [10]. According to Mondal et al [15] annual total rainfall has increased by 4.960 mm/year and average temperature 0.005°C/year during the year 1960 to 2012 in Khulna. Besides this, the city people have been facing a groundwater crisis [16], massive water logging [17,18] and many other environmental problems. In this backdrop, the study of environmental risk profile of a city unit in Khulna city would broaden our understanding about the risk of Khulna city.

Environmental profiling is the method of assessing both physical and meteorological conditions; changes in other environmental phenomena are also assessed while developing such profile [19]. This study aimed to do environmental risk assessment through assessing the change in physical and meteorological conditions for the period 2003 to 2019. Though few studies have described the rainfall and the temperature change trend of KCC [15, 25] but no study has been conducted on LST, NDVI, NDMI, NDBI, slope, and topographical dynamics in Khulna

Article history:
Received 23 April, 2020
Received in revised form 15 July, 2020
Accepted 30 July, 2020
Available online 15 August, 2020

Corresponding author details: M.N. Haque
E-mail address: nhaque13@urp.kuet.ac.bd
Tel: +880 1681934283

city. This study considered all the gaps of previous researches. Therefore, this study puts emphasis on those important criteria which are directly/indirectly related to the urban risk and hazards. The outcome of the study signifies the importance of planned urbanization for the sound and healthy environment.

Study Area: Khulna, 3rd largest metropolitan of Bangladesh, situated in the south-west corner of the country. Sundarban, the largest mangrove forest (140,000 ha) and one of the UNESCO World Heritage Sites in the world located in this division [26]. Khulna City Corporation (KCC) located between 24°45' and 24°54' northern latitudes and in between 89°28' and 89°35' east longitudes [27] and lies at 12ft above mean sea level with 657798 populations in 45.154 sq.km area [28]. The KCC consist of 31 wards where the population density is 20113 persons/sq.km (BBS 2015). Due to unplanned and haphazard urbanization, the environment of KCC has been observed an enormous change since 2000 [25]. Population growth has resulted in the rapid land cover change in Khulna.
The study area, KCC Ward 01 and Ward 03 were selected (Fig. 1) from Khulna City Corporation area having total population 18900, 21821, density 1032, 5436 per sq.km (BBS 2011) respectively. The area consists of mainly three land cover type such as Residential, Industrial and Agricultural. Most of the land is used for vegetation and agricultural purpose. Still ward 1 and 3 are supposed to be good in environmental perspective, because these wards cover relatively more environmentally friendly land cover types (such as vegetation, agricultural land and waterbodies) and have

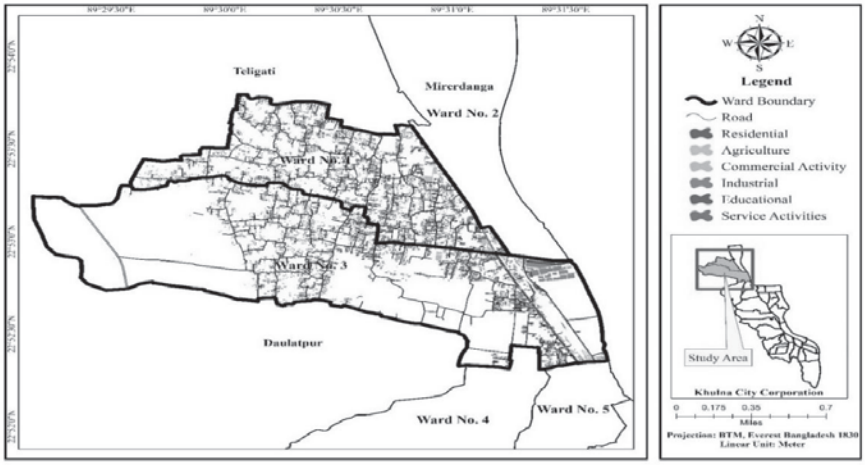

Fig. 1: Location of study area map. (Source: KDA, 2020).

less population than other wards. As both the wards have residential and industrial areas at the same time, it is necessary to identify the risk zones by investigating the environmental circumstances in here. That's why KCC ward no 1 and 3 were chosen as the study area in this research.

Materials & Method: Among 31 KCC wards, ward 1 and 3 were selected as study unit/area focusing on the continuous land cover change and due to the existence of two sensitive land use type (residential and industrial areas) within the same place side by side. The field of research was chosen to identify environmental changes such as topological dynamics, meteorological dynamics and surface dynamics in the study area. Land use, Topography [20] (Slope, Elevation, Contour), Land Surface Temperature (LST), Healthy Vegetation (NDVI), Soil Moisture (NDMI), Density of Buildup land (NDBI), etc. were considered as surface dynamics while the atmospheric temperature, relative humidity, and annual total rainfall were considered as meteorological dynamics in this research. Several factors influence the adverse environmental change. The LST, atmospheric temperature, annual rainfall, humidity, vegetation, soil moisture, buildup environment, LULC change was considered as the influencing factor by reviewing previous researches [38]. The type of vegetation determines the root system, the quantity, and

quality of plant residues entering the soil, as well as how those plant residues enter the soil. The restoration of vegetation is an important measure for soil and water conservation engineering and environmental reconstruction. Two Multi-spectral Landsat images (Landsat 5 TM for 2003 and Landsat 8 OLI for 2019) were collected from the United States Geological Survey (USGS) to measure the LULC, LST, NDVI, NDMI and NDBI dynamics in the study area (Table 1). These three satellite images collected were taken in the same month (April) to avoid the seasonal effects. Due to less possibility of rainfall in Khulna during April, the accuracy or acceptability of LST result is higher than in other months. The maximum cloud coverage was set less than 10% during collecting the images and the images were of 30m resolutions and the path was 138 and the row was 44 for both images.

Table 1. Spectral Band used to calculate different indicators.

Indicators	Landsat 5 (TM)		Landsat 8 (OLI)	
	Band Number	Band Name	Band Number	Band Name
LULC	Band 1, Band 2, Band 3, Band 4	Blue, Green, Red, NIR	Band 2, Band 3, Band 4, Band 5	Blue, Green, Red, NIR
LST	Band 6	Thermal	Band 10	Thermal
NDVI	Band 3 and Band 4	Red and NIR	Band 4 and Band 5	Red and NIR
NDMI	Band 4 and Band 5	NIR and SWIR	Band 5 and Band 6	NIR and SWIR
NDBI	Band 4 and Band 5	NIR and SWIR	Band 5 and Band 6	NIR and SWIR

Source: USGS, 2020

The study also analyzed the time series of meteorological data in the study area. Such as the trend analysis of annual total rainfall, relative humidity, the average and maximum temperature in the study area from 2003 to 2019. These data were collected from the Bangladesh Meteorological Department (BMD), Khulna station.

LULC Classification: Landsat 5 (TM) and Landsat 8 (OLI) images which have 30m resolution were used in ERDAS Imagine 2014 and ArcGIS 10.7 version for the year 2003 and 2019 to identify the Land use and Land Cover (LULC) types in the study area. The land cover type has been classified into five categories (buildup area, vacant land, agricultural land, water bodies, and vegetation) by applying maximum likelihood supervised classification method [29, 30] to identify the land cover pattern. The atmospheric and radiometric correction was performed to enhance the spatial resolution and to fix the error of the raster images[24]. Elevation, Slope, Contour analysis was conducted to assess the topographic scenario of the selected study area. The elevation data is generated from the Google Earth Engine platform (Google Earth Pro) using ArcGIS 10.7 version.
To check the accuracy of the classification, more acceptable and better quantitative image classification accuracy measurement technics named Kappa statistics and confusing matrix were calculated following the literature [31, 32, 13].

Normalized Difference Vegetation Index (NDVI): Normalized Difference Vegetation Index (NDVI) was used in the study by using a near-Infrared spectral band and a Red spectral band of Landsat's multi-spectral sensor [22]. NDVI is estimated based on the absorption of radiation in the red (R) spectral band and the maximum reflection of radiation in the near-infrared (NIR) spectral band [33].

$$NDVI = (NIR\ Band - Red\ Band)/ (NIR\ Band + Red\ Band) \quad \text{eq.1}$$

NDVI was estimated temporally to understand the change of land cover during the study period. The NDVI is widely used in many research project conducted earlier for measuring vegetation cover. The value of NDVI ranges from -1.0 to +1.0 whereas very low values of NDVI (-0.1 and below) correspond to barren areas of rock, sand, or urban/built-up. Zero indicates the water cover. Moderate values represent low density of vegetation (0.1 to 0.3), while high values indicate dense vegetation (0.6 to 0.8) [33].

Normalized Difference Moisture Index (NDMI): Normalized Difference Moisture Index (NDMI) was used to calculate the amount of moisture or water bodies presence on the land surface. NDMI index can regulate irrigation in real-time, greatly enhancing agriculture, particularly in areas where it is difficult to meet water needs [13]. NDMI is the ratio of the difference and the sum of the near-infrared and SWIR refracted radiation of the Landsat Multi-spectral sensor [34].

$$NDMI = (NIR-SWIR)/(NIR+SWIR) \quad \text{eq. 2}$$

NDMI is a dimensionless quantity that has ranged from -1 to + 1. The higher value indicates the higher amount of water content, sufficient moisture, and the lower value indicates the least amount of water content, water stress on the land surface [35].

Normalized Difference Buildup Index (NDBI): Normalized Difference Buildup Index (NDBI) represents the density of the build-up area on the land surface from the ratio between the difference and the sum of the near-infrared and SWIR refracted radiation of Landsat Multi-spectral sensor using the following equation [36].

$$NDBI = (SWIR -NIR)/ (SWIR +NIR) \quad \text{eq. 3}$$

NDBI value varied from -1 to + 1. The higher value indicates the density of Buildup land or the urban area or developed area and the lower value indicates the less Buildup or rural area or undeveloped area [13]. Three indices NDVI, NDMI, and NDBI were used in this analysis to distinguish the LULC types by setting the correct threshold values. It should be noted that these indices can have different values for various types of land cover, depending on the study areas, the time of image acquisition, and specific atmospheric and precipitating conditions. The higher value of NDVI and NDMI indicates environmentally friendly areas whereas the higher value of NDBI suggests the risky areas in a zone.
For the better visualization of NDVI, NDMI, and NDBI in the map, the value of these indices was categorized into five different classes and the value range is shown in table 2.

Table 2. Land use Indices value range according to the classified category.

Categories	NDVI	NDMI	NDBI
Very Low	-0.216 to -0.067	-0.387 to -0.235	-0.387 to -0.235
Low	-0.067 to 0.080	-0.235 to -0.083	-0.235 to -0.083
Moderate	0.080 to 0.228	-0.083 to 0.067	-0.083 to 0.067
Medium	0.228 to 0.377	0.067 to 0.219	0.067 to 0.219
High	0.377 to 0.525	0.219 to 0.371	0.219 to 0.371

(Source: Author, 2020)

Land Surface Temperature (LST): LST is the radiative surface temperature of the soil surface which plays a vital role in the physics of the land surface through the energy cycle and the exchange of water with the atmosphere [36]. The estimation of LST from satellite thermal data includes several procedures such as sensor radiometric calibration, correction of atmospheric and surface emissivity, characterization of land-cover spatial variation etc. In this study, the LST of the study area was determined to explore the current environmental condition of the study area. The authors are referred to the literature [26, 13, 22] for the details of the process for the derivation of LST from Landsat images.

$$L\lambda = AL + ML \times QCAL \quad \text{eq. 4}$$

Where, $L\lambda$ = TOA Spectral Radiance ($W/(m2 \times sr \times \mu m)$), ML = Radiance multiplicative scaling factor for the band, AL = Radiance additive scaling factor for the band, QCAL = the quantized calibrated pixel value in Digital

Numbers (DN)In the second step the TOA spectral radiance (Lλ) values is converted into another variable called At-Satellite Brightness Temperature (TB)

$$TB = K2 /(\ln(K1 /L\lambda + 1) \quad \text{eq. 5}$$

Where, TB =At-Satellite Brightness Temperature, in Kelvin (K)K1, K2 = Thermal conversion constants for the band. Finally, the TOA Brightness Temperature was converted to LST values.
Where, LST = Land Surface Temperature in Kelvin (K), λ = the wavelength of emitted radiance,
α = hc/k (1.438 × 10-2 mK), h = Planck constant (6.626 × 10-34 J s-1), and c = velocity of light (2.998 × 108 m s-1), k = Boltzmann constant (1.38 × 10-23 J K-1), ε = surface emissivity, calculated according to equation (5)

$$LST = [TB/ (1 + (\lambda \times TB/ \alpha)) \times \ln \varepsilon] \quad \text{eq. 6}$$

$$\varepsilon = (0.004 \times Pv) + 0.986 \quad \text{eq. 7}$$

Where, Pv is the vegetation proportion calculated following equation

$$Pv = [(NDVI - NDVImin) / (NDVI - NDVImax)]2 \quad \text{eq. 8}$$

To obtain the land surface temperature values in Celsius (°C), 273.15 was extracted from the initial values (K). LST has adverse impacts on the environment and global warming, that's why the higher value of LST considered as the risky areas in the weighted overlay method.

Weighted Overlay Method: Weighted Overlay method is applied to a specific metric scale of values to different and dissimilar inputs to produce an optimized study. The Weighted Overlay method (WOM) is one of the most commonly applied methods for overlay studies to address multi-criteria problems such as site selection and suitability models [23]. In this study, WOM has been chosen to identify the hazardous area or risk zone detection. The Weighted Overlay method has been used for modeling, hazardous zone identification where higher values usually mean a more risk zone or hazardous area, whereas the lower values indicate a low-risk zone area. In this method, the raster datasets need to be reclassified into different classes to convert floating-point raster to integer raster before applying the "Weighted Overlay" tool. A new value is added to each value class in an input raster, depending on a scale of assessment. Such current values are reclassifications of the initial raster values for inputs. As this study is applied GIS and Remote Sensing approach in WOM to prepare hazard maps, more importance has been given on land use and satellite image-based factors. Here Table 3 shows the influence of different factors for the WOM.

Table 3. Influence percentage of different criteria.

Criteria	Influence in percentage
Elevation	12
Slope	8
LST	30
NDVI	17
NDBI	20
NDMI	13

Source: Expert Opinion, 2020

Results and Discussion:

Accuracy Assessment: Table 4 represents the overall accuracy of the maximum likelihood supervised image classification method. The value of the overall accuracy is 92.13% and 94.67% for the years 2003 and 2019 respectively and the Kappa coefficient values are 0.9014 and 0.947 which indicates better accuracy of the classified data and suitable for urban expansion detection [31, 32, 38].

Table 4. Overall accuracy assessment value and Kappa Coefficient.

LULC Accuracy	2003		2019	
	Producer's	Users	Producer's	Users
Buildup	84.7%	98.57%	100.00%	87.50%
Agricultural Land	92.00%	89.99%	100.00%	100.00%
Vegetation	88.89%	100.00%	100.00%	95.30%
Vacant Land	99.00%	80.00%	83.33%	100.00%
Waterbodies	100.00%	84.00%	100%	100.00%
Overall Accuracy	92.13%		94.67%	
Kappa Statistics	0.9014		0.947	

Source: Authors calculation, 2020

LULC Identification and Change Analysis: To identify the Land use and Land cover of the study area, the supervised image classification method has been conducted using spectral band "Blue", "Red", 'Green", "Near Inferred" of Landsat Satellite Imagery (Landsat 5 (TM) & Landsat 8 (OLI) for the year 2003 & 2019 respectively) through ERDAS Imagine 2014 and ArcGIS 10.7. The LULC has been categorized into five categories such as Buildup, Agricultural, Vacant, Vegetation, and Waterbody. Fig. 2 visualizes the comparative Land use and Land Cover Changes from the year 2003 to 2019 of KCC Ward 01 & Ward 03 of Khulna.

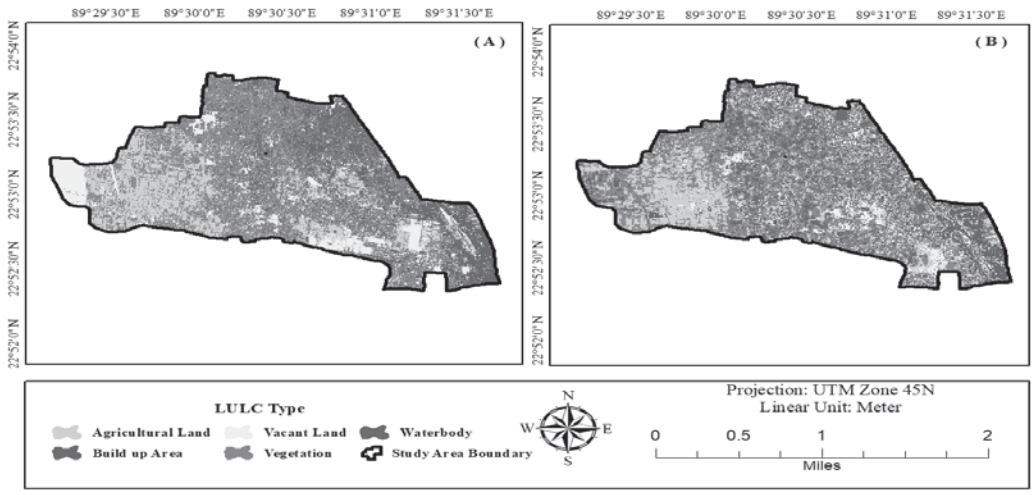

Fig. 2: Land use and Land cover scenario of KCC Ward 01 & 03 (Source: Author, 2020).

GIS-based satellite image classification for the year 2003 and 2019 illustrates the increase of agricultural land from 22% to 26%, buildup area 14% to 25% while the decrease of vacant land from 12% to 9%, vegetation 43% to 36%, and waterbody 8% to 5% in the study area (table 5). Population growth and unplanned urbanization have resulted in this massive change of landform in the study area. Due to the construction of residential houses and industries, the adverse reflection has been observed on vacant land, water bodies, and vegetation land cover in the study area. Fig. 3 shows the land cover change direction during the year 2003 to 2019. From the spatial analysis, it is found that agricultural land and build-up areas have increased by 3% and 11% respectively. At the same time, the amount of vegetation, vacant land, water body areas have decreased by 8%, 3% & 3% respectively in the last 16 years. As a consequence of urban expansion, rising population pressure, increasing housing demand, the dependency of wood fuel influenced the transformation of the vegetation, water bodies, and vacant land cover at a noticeable rate at KCC Ward 01 and Ward 03. From the field survey, it was found that several residential, industrial, educational,

commercial buildings and roads have been constructed in the study area during the study period which has influenced this rapid transformation of vacant property, water bodies, and vegetation land cover.

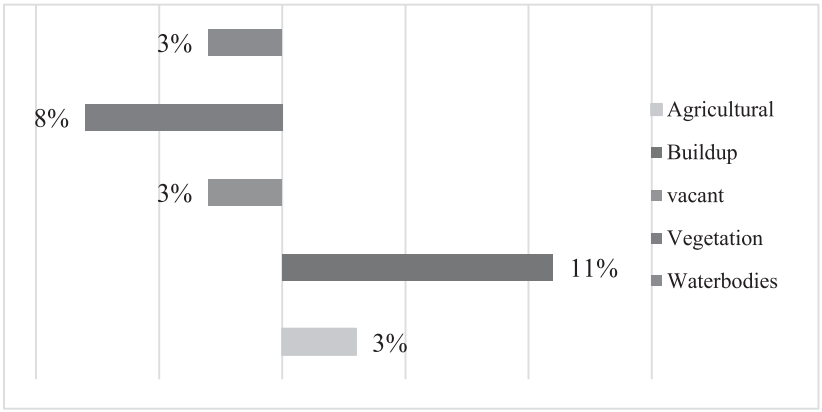

Fig. 3: Land cover change direction analysis during 2003 to 2019. (source: Authors' calculation, 2020).

The land cover change direction analysis in Fig. 3 shows the increase of buildup areas and agricultural areas by 11% and 3% which has resulted in the transformation or declination of water bodies, vacant land, and vegetation land cover types into agricultural land and buildup area. Fig. 2 visualizes the dense agricultural and vegetation land cover in the western portion and build up areas in the eastern portion of the study area.

Table 5. Comparative Land Cover type scenario from the year 2003 to 2019.

Year	2003		2019	
Land Use	Area in Acres	Percentage	Area in Acres	Percentage
Agricultural Land	323.89	22%	369.69	26%
Build Up Area	204.86	14%	360.88	25%
Vacant Land	171.78	12%	123.47	9%
Vegetation	627.40	43%	513.06	36%
Water body	116.20	8%	77.03	5%
Total	1444.14	100%	1444.14	100%

Source: Authors' calculation, 2020

Topographical Dynamics

Change in Elevation and Slope: The elevation of a geographical position is its height above or below from mean sea level, which measures in meters or foot unit as well as is also represented in the map by contour lines. The contour lines link points of the same elevation (called Contour Interval) or numbers representing the precise elevations of different points on the surface of the planet. The elevation data was derived from the Google Earth Engine utilizing ArcGIS technologies by developing a Digital Elevation Model (DEM) in Fig. 4. The lowest and maximum height in 2019 is 0.38 m and 12.49 m respectively but at KCC Ward 01 and Ward 03 in 2003 it was 0.28 m and 12.90 m respectively. It is observed that over 16 years the average elevation was changed from 6.60 m to 6.43 m, which means that the average elevation was lowered by 0.17 m. It has improved owing to climate change that has been affected by the increasing sea level and air temperature. Continuous improvements in the soil-sheets, such as the development of new infrastructure, residential building, and ground cut-filling. The Khulna division is situated in the coastal area next to the Bay of Bengal, and this negative shift has increased the probability of flooding, long-term water lagging that decreases the productivity of the agricultural property as well as influences the local climate of the study urban units.

The slope dataset was prepared from the Digital Elevation Model (DEM) utilizing GIS technology in ArcGIS 10.7, which helps to identify the study area's dynamic slope over 16 years. The extracted slope was classified into 4 classes using the equal interval classification method in the ArcGIS 10.7 version. A land's gradient or inclination is the percentage increase in its elevation for a certain period. Fig. 5 visualizes that almost 32% of the area was on the lower slope, 23% moderate, 22% average, and 23% high slope region in 2003 while in 2019 it has improved to 41% lower, 19% moderate, 20% average and 20% high slope zone. Because of the dependency on the elevation, the slope change has noticed over the 16 years of the study period. This study interprets that from 2003 to 2019 there was a rise of 9% of the lower land area, which raised the risk of going submerged in rainy season triggering floods and hazardous to study area.

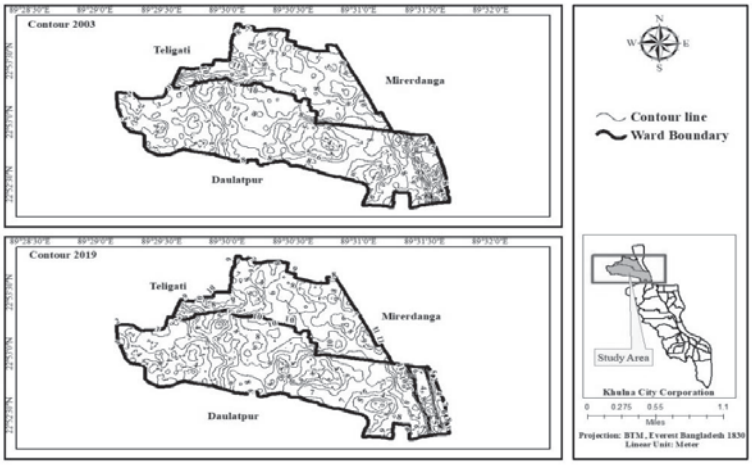

Fig. 4: Comparative Contour map from 2003 to 2019 at study area (Source: Author, 2020).

Fig. 5: Comparative slope change analysis for the year 2003 and 2019. (Source: Author 2020)

Meteorological Dynamics: In this study, from the year 2003 to 2019, three forms of environmental changes such as temperature, rainfall, and relative humidity change trend analysis was conducted by using the data collected from BMD to examine the meteorological dynamics during the study period. Since there is only one weather station in Khulna City, the data for all locations in Khulna City would be the same.

Alternation of Annual Rainfall and Relative Humidity: The annual total rainfall in the study area indicates a decreasing pattern (Fig. 6a) over 2003-2019. Data reveals that over the last 16 years the average annual total rainfall

was 1868.941mm whereas it was measured 1789.786mm. The average monthly rainfall was measured 155.75mm during the study period. Though the amount of annual total rainfall was measured more in the study year than the year 1990 to 2000, the trend analysis in Fig. 6a shows a negative annual trend since 2003. The highest rainfall measured 2668 mm in the year 2007 and the lowest total rainfall 1357mm in the year 2010 in the study area. The R^2 value of the annual trend analysis was found to be 0.012.

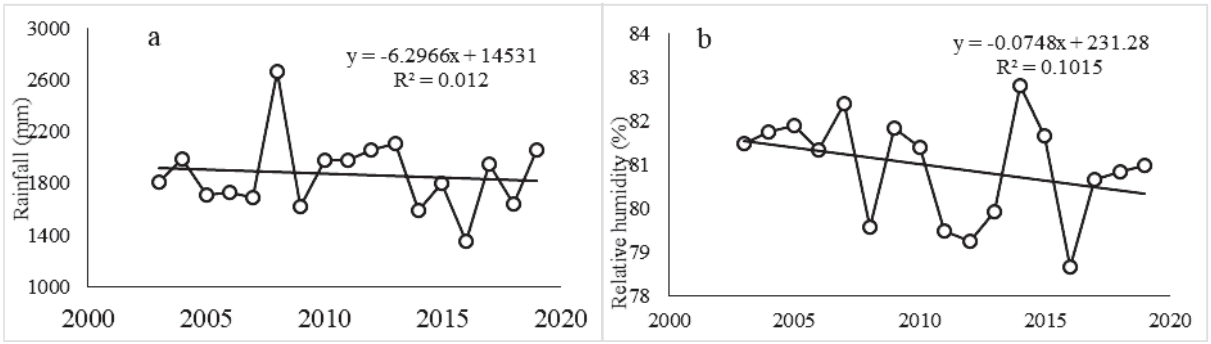

Fig. 6: Meteorological data trend analysis (a) annual total rainfall (b) relative humidity during 2003 to 2019 (Source: BMD, 2020).

Average relative humidity trend analysis in Fig. 6b shows the decreasing trend in the study area during the study period. The average relative humidity was measured 80.95% during the year 2003 to 2019 whereas it has been 80.58% since 2000. The highest relative humidity measured 82.83% in 2014 and the maximum humidity was measured 91% in September 2007. BMD data analysis shows that the average humidity in the study area remains between 72% to 79% from January to May and 79.8% to 87.4% from June to December. The coefficient of determination, R^2 value was found 0.1015 for relative humidity trends in the study area during the study period. This decreasing rate indicates a positive environmental change in the study area.

Temperature Profile Analysis: To illustrate the atmospheric temperature conditions in the study area, the trend analysis of minimum and the maximum temperature has been conducted. Both the average minimum (Fig. 7a and maximum (Fig. 7b) shows the increasing trend of temperature during the study period. The highest average maximum temperature was observed 32.07^0C in 2018 and the maximum temperature was observed 40.7^0C in May 2014 in the study area. The lowest average minimum temperature was observed 17.57^0C and the minimum temperature was observed 8^0C in January 2018. The increasing trend of atmospheric temperature indicates the adverse environmental change in the study area. The coefficient of determination value of both average maximum and minimum temperature was found 0.1769 and 0.0026 respectively in time series temperature trend analysis for the year 2003 to 2019 in Khulna.

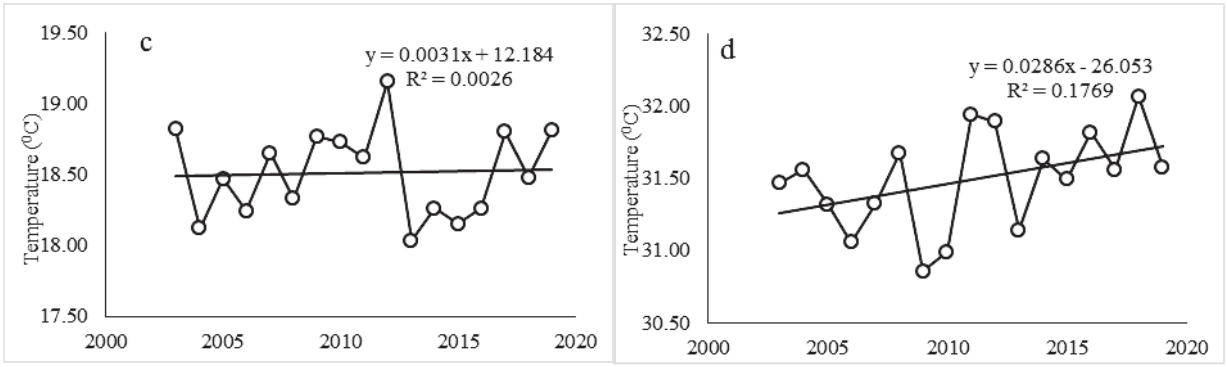

Fig. 7: Temperature change trend analysis (a) average minimum temperature (b) average maximum temperature during the year 2003 to 2019. (Source: BMD, 2020).

Transition of LST: The surface temperature of the study area was calculated by using equation 4-8 for the year 2003 and 2019 using the Thermal Spectral band of Landsat 5 (TM) and Landsat 8 (OLI) respectively in ArcGIS. Fig. 8 shows the increase of minimum surface temperature by 1.370C during the study period. The surface temperature value range was derived between 23.25^{0}C to 31.20^{0}C in 2003 and 24.62^{0}C to 30.96^{0}C in 2019. The percentage of land cover with a higher LST value of more than 29^{0}C has been increased in the study area. The average LST was increased at a rate of 0.125^{0}C / year. The analysis shows that about 55.81% of land cover had the LST value less than 25^{0}C in 2003 but in 2019 it decreased to only 0.11% of total land cover. The percentage of land cover in the LST value range 27^{0}C to 29^{0}C has been increased from 9.56% to 26.53% during the study period.

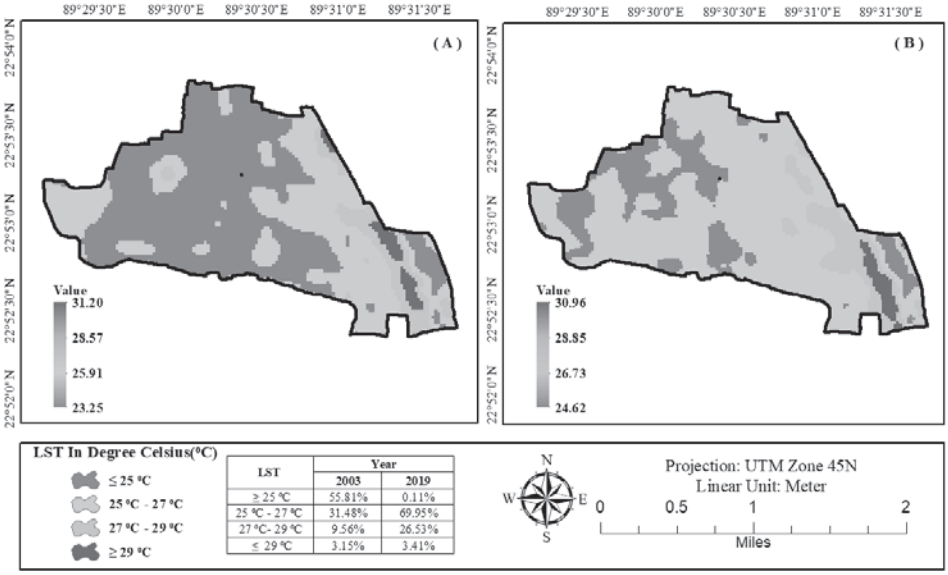

Fig. 8: Visualization of surface temperature in the study area in the year (A) 2003 and (B) 2019.

Comparing the LST value of two different years in Fig. 8, it can be concluded that even though the maximum LST value has been decreased, but the average surface temperature and the percentage of land cover with higher LST value have been increased during the study period. Decrease of water bodies, vacant land, and vegetation land cover and their transformation to build-up areas has resulted in the increase of average surface temperature and the percentage of area with higher LST value.

Land-use Indices Analysis:

Vegetation Health Analysis: Normalized Difference Vegetation Index (NDVI) was calculated using the spectral band of Landsat 5 (TM) and Landsat 8 (OLI) for the year 2003 and 2019 respectively through ArcGIS following equation 1. The maximum NDVI value suggests thick and balanced vegetation, while the lowest value shows weak density and unhealthy vegetation [37]. The NDVI raster dataset was categorized into five groups (Fig. 9) based on their value ranges accompanied by an equal interval classification method in ArcGIS to explain clearly what the NDVI rasters represent to us. The sum of healthy vegetation has been decreased slowly from the year 2003 to 2019 as illustrated in Fig. 9. This raster-based study reported that in 2003 land occupied by the high dense vegetation was 41%, but in 2019 it dropped to approximately 20%. It happened due to the continuing transition of vegetation to different land use in the study area (table 4 and Fig. 3).

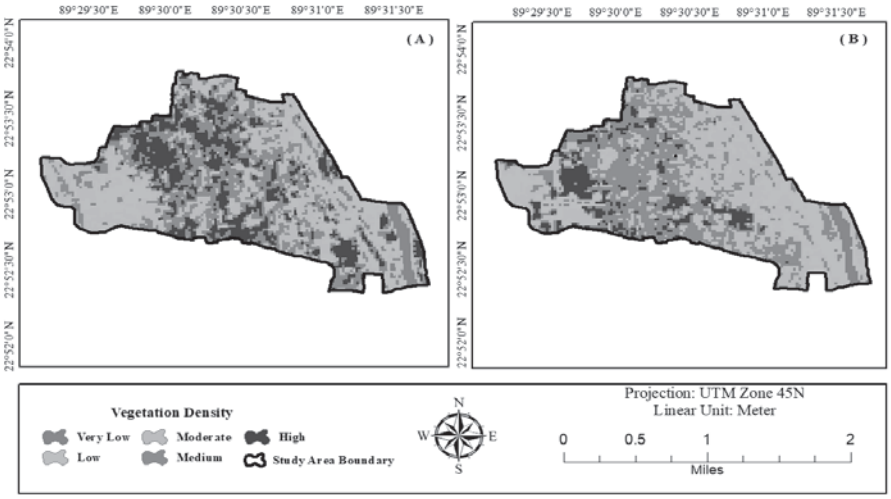

Fig. 9: Visualization of derived NDVI map for the year 2003 and 2019. Author, 2020.

Moisture Profile Analysis: The NDMI raster dataset has been categorized into five classes (table 2, Fig. 10) according to their value ranges accompanied by an equal interval classification method using ArcGIS to visualize the moisture conditions of the study area. As shown in Fig. 10, the amount of the concentration of balanced moisture on the land surface gradually declined from 2003 to 2019. This raster-based analysis shows that about 84% of land filled with balanced and moderately balanced moisture in 2003. In 2019, the amount of balanced moisture land cover reduced to 60%. The transformation of water bodies in the buildup area and decreasing trend of rainfall has resulted in the reduction of soil moisture in the study area. Over 16 years, water bodies have been converted into the buildup area, barren field, plantation field, and agricultural property, meaning that about 28% of the water bodies have shifted to farmland, 20% to build up, 40% to vacant land, 9% to the plantation. This propensity to decrease waterbodies in the study area is a source of disturbance of the water ecosystem and will cause long term water lagging during the rainy season of the study area.

Buildup Area's Scenario: The maximum NDBI value suggests the presence of a higher concentration of buildup areas, while the lowest NDBI value indicates the lowest concentration or absence of the buildup area [36]. The derivation of NDBI using equation 3 in Fig. 11 shows the amount of the concentration of highly buildup area on land surface is rapidly increased during the year 2003 to 2019. NDBI in Fig. 10 shows that the percentage of areas with low and medium NDBI values was most in 2003. But an increase of 11% buildup areas (Fig. 3) and transformation of vegetation and water bodies has resulted in the increase of areas with moderate median and higher NDBI value in the study area in 2019. From the field survey, it is found that many residential buildings and other industries were established in the study area, which has influenced the increase of NDBI values in the study area.

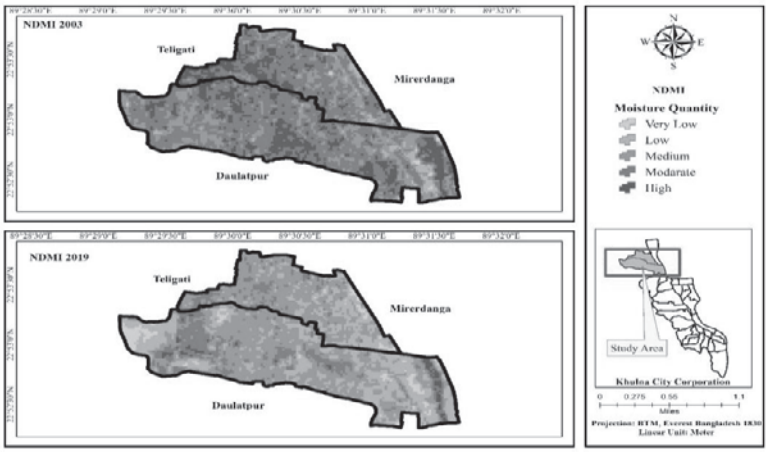

Fig. 10: Visualization of derived NDMI map for the year 2003 and 2019. Author, 2020.

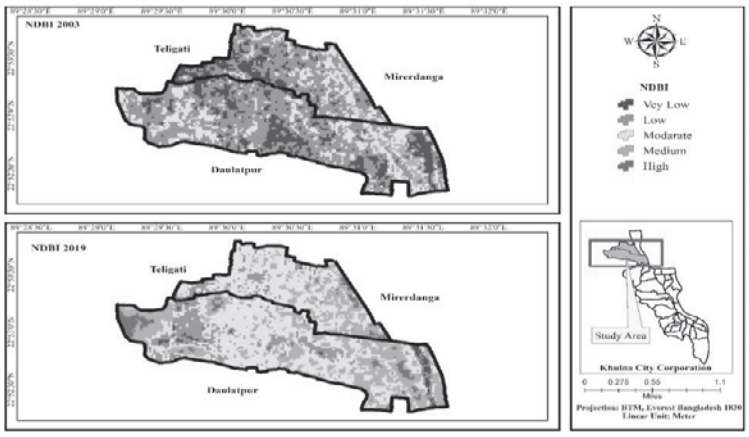

Fig. 11: Visualization of derived NDBI map for the year 2003 and 2019. Author, 2020.

Identification of Hazard Zone: The "Weighted Overlay Method" has been used to prepare the hazard zone map in ArcGIS to define the risk severity areas as well as to measure the comparative risk level in the study area. Factors which impact the environment such as elevation, slope, LULC, NDVI, NDMI, NDBI, and their transition were accounted for. Fig. 12 outlined the spatial aspect of risk intensity on a map where the hazard scenario was illustrated into three risk levels (high, low, medium). The presence of a sufficient amount of vegetation, water bodies, rainfall, LST, and other influencing factors have been taken into account to categorize the risk level. The low-risk level indicates the presence of a sufficient amount of vegetation, water bodies, truncated buildup areas, and has no significant impact on environmental change. The medium and high level of risk indicates an insufficient amount of vegetation, water bodies, rainfall along with dense buildup areas from head to foot, higher LST values, and other influencing factors in table 3. The outcome of the study demonstrated that the areas under low-risk level were 39% in the year 2003, 58% in a medium-risk level and 3% in the high-risk level (Fig. 12). While in 2019 it is seen that 35% of areas are in the lower-risk level, 59% are under medium risky area, and 6% under high-risk areas (table 5). Within 16 years the high-risk level areas have been increased by 3% (table 5) which suggests that the risk level is increasing day by day, which can bring danger to the ecosystem a well as our living environment. Moreover, the study demonstrated the hazardous environment of the study area due to unplanned urban expansion, i.e. expansion of residential and industrial areas together in a small area.

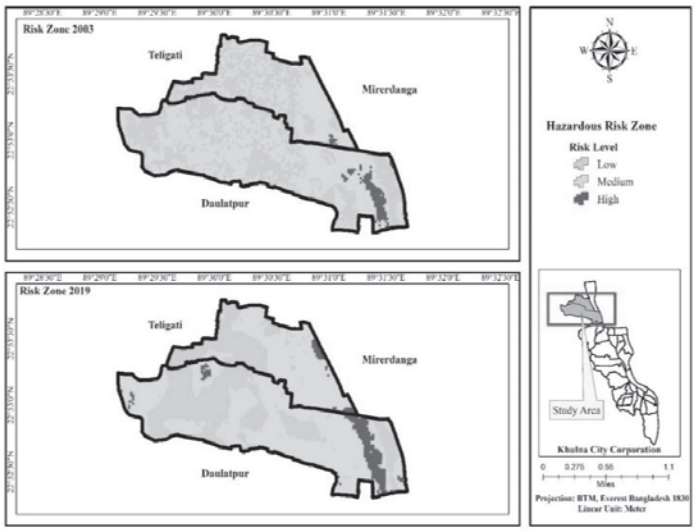

Fig. 12: Spatial location of the hazardous/risky area during 2003 and 2019 in the study area (Source: Author, 2020).

Table 5. Outcomes of risk level assessment of the study area.

Risk Level	Area in Percentage	
	2003	2019
Low	39%	35%
Medium	58%	59%
High	3%	6%

Source: Author's calculation 2020

Conclusion: The rapid transformation of an area land cover in an unplanned manner significantly affects the climate resulting in atmospheric temperature change, soil erosion, humidity change, an increase of soil salinity, rainfall change, topographical change, and causes an environmental hazard. This study has accounted for several meteorological, topographical, and man-made issues to identify the hazardous areas in the study urban unit. The analysis shows the transformation of 8% vegetation, 3% water bodies, and 3% vacant land into 11% buildup and 3% agricultural land over the study period. Expansion of housing area and the establishment of new infrastructure have influenced this change. The average elevation of the study area lowered by 0.1m and 40% areas of the total study area were found in the lower slope region in the year 2019. The outcome of the meteorological analysis shows the decreasing trend of annual total rainfall and relative humidity whereas the increasing trend of minimum and maximum temperature. The increase of surface temperature by 2℃ and areas with higher LST values has resulted in an increase of higher-level risk zones in the hazard map. Though still, 59% of the study area remained under medium risk zones, the LULC transformation rate, LST change, and other factors prognoses the increase of the higher risk zone areas in the study area. Several criteria have been analyzed to describe the environmental, geographical, and physical conditions of the study area. But there are some limitations of the study. The study used only six factors to prepare hazard maps for the study area but there are some other factors such as flood, drought, groundwater level, etc which are not considered in this study. The WOM is a raster-based analysis tool that is used in this study. Landsat satellite images were used in this study to derive LULC, LST, NDVI, NDMI, and NDBI values in the study area but the size of the study area is relatively small. For this, the accuracy assessment has been conducted for the whole KCC area although that will no change much in the case of the study area.

The overall study signifies the importance of planned urbanization in any area to mitigate adverse environmental impacts. This study will further help to identify and locate the hazardous/risky areas of any region on the map and will help policymakers to take the necessary steps to reduce these adverse environmental impacts.

References:

[1] A. M. Amera and B. Tefera, The role of Environmental Impact Assessment for sustainable development. In: IAIA13 Conference At: Calgary Stampede BMO Centre, Calgary, Alberta, Canada, 2013.

[2] J. J. Arsanjani, M. Helbich and E. d. N. Vaz, Spatiotemporal simulation of urban growth patterns using agent-based modeling: The case of Tehran, Cities. 32 (2013) 33-42.

[3] W.L. Filho, A. Balogun, O. E. Olayide, U. M. Azeiteiro, D.Y. Ayal, P. D. C. Muñoz, G. J. Nagy, P. Bynoe, O. Oguge, N.Y. Toamukum, M. Saroar, C. Li, Assessing the impacts of climate change in cities and their adaptive capacity: Towards transformative approaches to climate change adaptation and poverty reduction in urban areas in a set of developing countries. Science of The Total Environment. 692 (2019) 1175-1190. https://doi.org/10.1016/j.scitotenv.2019.07.227.

[4] R. F. M. Ameen and M. Mourshed, Urban environmental challenges in developing countries—A stakeholder perspective, Habitat International. 64 (2017) 1-10.

[5] A. H. U. Zaman, K. M. T. Alam and M. J. Islam, Urbanization in Bangladesh: Present Status and Policy Implication, ASA University Review. 2 (2010) 1-16.

[6] M. A. Ali, Unplanned urbanization of Dhaka city: increase of rainfall induced flood vulnerability, BRAC University, Dhaka, Bangladesh, Dhaka, 2006.

[7] B. Ahmed, M. Kamruzzaman, X. Zhu, M. S. Rahman and K. Choi, Simulating Land Cover Changes and Their Impacts on Land Surface Temperature in Dhaka, Bangladesh, Remote Sensing. 5 (2013) 5969-5998.

[8] N. S. Parvin and D. Abudu, Estimating Urban Heat Island Intensity using Remote Sensing Techniques in Dhaka City, International Journal of Scientific & Engineering Research. 8 (2017) 289- 298.

[9] S. Labib, M. N. Neema, Z. Rahaman, S. H. Patwary and S. H. Shakil, Carbon dioxide emission and bio-capacity indexing for transportation activities: A methodological development in determining the sustainability of vehicular transportation systems, Journal of Environmental Management. 223 (2018) 57-73.
[10] M. Hasanuzzaman, M. Hossain, M. Saroar, Diversity and preference of agricultural crops in the cropland agroforests of southwestern Bangladesh, International Journal of Agriculture and Crop Sciences. 7 (2014) 364-372.
International Conference on Climate Change Impact and Adaptation, Gazipur, Bangladesh, 2013.
[12] UNICEF, Learning to Live in a Changing Climate: The Impact of Climate Change on Children in Bangladesh, United Nations Children's Fund (UNICEF), 2016.
[13] A. A. Kafy, A.A. Faisal, M. M. Hasan, Abdullah-Al- Faisal, M. Islam and M. S. Rahman, Modelling future land use land cover changes and their impacts on land surface temperatures in Rajshahi, Bangladesh, Remote Sensing Applications: Society and Environment. 18 (2020).
[14] N. B. Nazir and N. A. Tonoy, An Analysis on The Vulnerable Effect of Climate Change on Children & Adaptation in Changing Situation in Darusha Union, Rajshahi District: Bangladesh. In: International Conference on Planning Architecture and Civil Engineering, Rajshahi, Bangladesh, 2019.
[15] K. K. Mondal, M. A. Akhter, M. Mallik and S. Hassan, Study on Rainfall and Temperature Trend of Khulna Division in Bangladesh, DEW-DROP. 4 (2017).
[16] S. K. Adhikary, M. Manjur-A-Elahi and A. M. I. Hossain, Assessment of Shallow Groundwater Quality from Six Wards of Khulna City Corporation, Bangladesh, International Journal of Applied Sciences and Engineering Research. 1(2012) 488-498.
[17] M. M. Rahman, A. Akteruzzaman, M. Khan, A. Jobber and M. Rahman, Analysis of Water Logging Problem and Its Environmental Effects Using GIS Approaches in Khulna City of Bangladesh, Journal of Socio. Res. Dev. 6 (2009) 572-577.
[18] S. K. Sarkar, M. A. Rahman, M. Esraz-Ul-Zannat and F. Islam, Simulation-based modeling of urban waterlogging in Khulna City, Journal of Water and Climate Change. (2020) 1-14.
[19] M. Kasparek and M. Dimashki, Country Environmental Profile for the Syrian Arab Republic. European Comission, 2009.
[20] A. Sharma and D. Gupta, Derivation of topographic map from elevation data available in google earth, Civil Engineering and Urban Planning: An International Journal. 1 (2014) 14-21.
[21] F. Esteban, A. Tassone, M. Menichetti and E. Lodolo, Application of Slope Maps as a Complement of Bathymetry: Example from the SW Atlantic, Marine Geodesy. 40 (2017) 57-71.
[22] G. Georgiana and B. Urițescu, Land Use/Land Cover changes dynamics and their effects on Surface Urban Heat Island in Bucharest, Romania, International Journal of Applied Earth Observation and Geoinformation. 80 (2019) 115-126.
[23] ESRI, Understanding Weighted Overlay. 2014. [Online]. Available: https://www.esri.com/about/newsroom/arcuser/understanding-weighted-overlay/. [Accessed 20 February 2020].
[24] Szabo S., Ahmad S., Adger W.N. Population Dynamics in the South-West of Bangladesh. In: Nicholls R., Hutton C., Adger W., Hanson S., Rahman M., Salehin M. editor. Ecosystem Services for Well-Being in Deltas. Palgrave Macmillan, Cham; 2018. pp. 349-365.
[25] M. A. Fattah, S. R. Morshed and M. N. Haque, Characteristics of current land use pattern of urban area A Case Study on Ward 24 (Nirala), Khulna City Corporation (KCC), Khulna, Bangladesh. In: 1st International Conference on Urban and Regional Planning. Dhaka, 2019.
[26] B. Ahmed, Modelling Spatio-Temporal Urban Land Cover Growth Dynamics Using Remote Sensing and GIS Techniques: A Case Study of Khulna City, Journal of Bangladesh lnstitute of Planners, 4 (2011) 15-32.
[27] M. N. Haque, M. A. Mamun, M. M. Saroar and T. K. Roy, Application of "DPSIR" Framework to Assess the Status and Role of Blue Ecosystem Services (BES) in Khulna City, Journal of Engineering Science (JES). 10 (2019) 49-60.
[28] M. S. Hossain, K. Roy and K. D. Datta, Spatial and temporal variability of rainfall over the south-west coast of Bangladesh, Climate. 2 (2014) 28-46.
[29] A. Z. Bishta, Assessment of the reliability of supervised classifications of Landsat-7, ASTER, and SPOT-5 multispectral data in rock unit discriminations of Jabal Daf-Wadi Fatima area, Saudi Arabia, Arabian Journal of Geosciences. 11 (2018) 755.
[30] F. E. Oliva, O. S. Dalmau and T. E. Alarcón, Lecture Notes in Computer Science (including subseries Lecture Notes in Artificial Intelligence and Lecture Notes in Bioinformatics). In: Mexican International Conference on Artificial Intelligence. MICAI 2014.
[31] R. G. Pontius and M. Millones, Death to Kappa: Birth of quantity disagreement and allocation disagreement for accuracy assessment, International Journal of Remote Sensing. 32 (2011) 4407-4429.
[32] K. Yadav and R. G. Congalton, Correction: Yadav. K. and Congalton. R. Accuracy Assessment of Global Food Security-Support Analysis Data (GFSAD) Cropland Extent Maps Produced at Three Different Spatial Resolutions, Remote Sensing. 11 (2019) 630.
[33] Y. Zhang, J. Gao, L. Liu, Z. Wang, M. Ding and X. Yang, NDVI-based vegetation changes and their responses to climate change from 1982 to 2011: A case study in the Koshi River Basin in the middle Himalayas, Global and Planetary Change. 108 (2013) 139-148.
[34] K. R. Ahmed and S. Akter, Analysis of landcover change in southwest Bengal delta due to floods by NDVI, NDWI and K-means cluster with landsat multi-spectral surface reflectance satellite data, Remote Sensing Applications: Society and Environment. 8 (2017) 168-181.
[35] H. Xu, Modification of normalised difference water index (NDWI) to enhance open water features in remotely sensed imagery, International Journal of Remote Sensing. 27 (2006) 3025-3033.

[36] Y. Zhang, I. O. A. Odeh and C. Han, Bi-temporal characterization of land surface temperature in relation to impervious surface area, NDVI and NDBI, using a sub-pixel image analysis, International Journal of Applied Earth Observation and Geoinformation. 11 (2009) 256-264.
[37] R. Chaudhari and D. Lal, Weighted overlay analysis for delineation of ground water potential zone: a case study of pirangut river basin, International Journal of Remote Sensing & Geoscience (IJRSG). 71 (2018).
[38] L. L. F. Janssen and F. J. M. V. D. Wel, Accuracy Assessment of Satellite Derived Land-Cover Data: A Review, Photogrammetric Engineering & Remote Sensing. 60 (1994) 419-426.
[39] M. Kumar, N. Mukherjee, G. P. Sharma and A. S. Raghubanshi, Land use patterns and urbanization in the holy city of Varanasi, India: a scenario, Environmental Monitoring and Assessment. 167 (2010) 417-422.